HETEROJUNCTION SOLAR CELL CALCULATIONS

by R. Sahai*

A. G. Milnes*

NGR-39-087-002

*Carnegie-Mellon University

Pittsburgh, Pennsylvania USA 15213

November, 1969

ABSTRACT

Solar cell efficiencies are computed for feasible semiconductor heterojunction cells of ZnSe-GaAs, GaP-Si, ZnSe-Ge and GaAs-Ge. The analysis includes the loss in efficiency because of reflection, incomplete collection and internal series resistance. Optimum antireflection films are also calculated. The results are compared with the performances expected of Si solar cells and GaAs homojunction cells.

ZnSe-GaAs cells are shown to have the potential for exceeding the efficiency of both Si and GaAs cells, if interface recombination losses are small. The output voltage, voltage regulation and temperature performance should be superior to that of Si cells. The window effect in the heterojunction cell may also provide some inherent resistance to deterioration under radiation conditions.

1. INTRODUCTION

The theoretical efficiencies for solar energy conversion using homojunction photovoltaic cells have been examined by numerous workers, including Rappaport and Wysocki (1961). Several possibilities for improving the conversion efficiency have been considered by Wolf (1960), such as multilayered cells (with more than one p-n homojunction in series) and heterojunction cells with the surface layer of a wide band-gap material. Kagan and Lyubashevskaya (1967) have given the results of computations for two-stage photocells with each stage operating in a separate circuit.

In homojunction cells, such as nSi-pSi, the silicon layer that receives the illumination must be quite thin so that carriers created just below its surface may have a reasonable chance of reaching the junction before recombination. The available output voltage is related to the energy gap of the silicon, and depends on the doping levels and on the lateral voltage drops that exist in the thin top layer under current flow conditions. In heterojunction solar cells, Perlman (1964) and others have shown that the output voltage is related to the energy gap of the base semiconductor, that is the one with the smaller of the two energy gaps. The semiconductor with the larger energy gap acts primarily as a window to photons of energy less than its band gap. However the advantage of the heterojunction cell is that this window layer may be proportioned in thickness and doping to minimize the lateral resistance losses in the cell.

In this study, theoretical computations of both maximum and practically attainable efficiencies for a number of feasible heterojunction cells, are presented. Sreedhar et al (1969) have recently considered the efficiency of heterojunction cells. However their calculations relate to ideal efficiencies and do not include many practical considerations that limit the performance.

In comparing and evaluating the results of various studies, it is important to know the assumptions made in arriving at the results. For example, it is usually assumed, except by Kagan et al (1967), that the reverse saturation current is governed only by the diffusion transport of minority carriers and that depletion layer generation components may be neglected.

In the present work, the following approach was taken:

(1) The heterojunction pairs considered were limited to those of close lattice match, and reasonably close thermal coefficients of expansion. Hopefully, therefore there is a chance that such heterojunctions may be made without the fabrication processes introducing high densities of interface states at the junctions. Recombination through interface states was assumed negligible in the results that follow.

(2) Some allowance was made in the calculations for the dependence of mobility and lifetime of carriers on doping levels in the semiconductor. Appendix A lists the values of various constants used in the computations.

(3) In heterojunctions there is normally an energy spike ΔE_c in the conduction band that is equal in principle to the electron affinity

difference of the two semiconductors. There is also a valence band barrier step ΔE_v, which is $(E_{g_1} - E_{g_2}) - \Delta E_c$, as shown in Fig. 1. For most heterojunction pairs ΔE_c is considerably less than ΔE_v. Therefore there are advantages in selecting for consideration n-window p-base heterojunctions. Then electrons flowing from the p base, where almost all the photon absorption takes place, are not seriously impeded by the relatively small ΔE_c spike. In the other class of heterojunction, p large-gap n small-gap, where the spike is ΔE_v and is large, it is usual to observe a great deal of interface recombination.

A second reason for the n-window p-base choice is that most of the current is caused by electrons collected as minority carriers from the narrow band-gap semiconductor, and the diffusion length of electrons tends to be appreciably more than that of holes in the semiconductors of interest to us.

(4) The diode equation was assumed to be of the type

$$J = J_{do} \left(e^{qV/kT} - 1\right) + J_{vgo} \left(e^{qV/2kT} - 1\right) \qquad (1)$$

where J_{do} and J_{rgo} are the diffusion and depletion layer recombination-generation components of the reverse saturation current. Their values are given by:

$$J_{do} = q\left(\frac{N_D D_n}{L_n \tanh(d/L_n)} e^{-q(V_D - \Delta E_c)/kT} + \frac{N_A D_p}{L_p \coth(t_I/L_p + \emptyset)} e^{-q(V_D + \Delta E_v)/kT}\right) \qquad (2)$$

$$\text{and } J_{rgo} = q\left(\frac{n_{i1}\, \ell_1}{2k_1 \tau_{o1}} + \frac{n_{i2}\, \ell_2}{2k_2 \tau_{02}}\right) \frac{1}{q\sqrt{V_D(V_D - V)}/kT} \qquad (3)$$

where N_D = donor concentration in the n-type material

N_A = acceptor concentration in the p-type material

V_D = built-in potential of the diode

ΔE_c = conduction band discontinuity expressed in volts

ΔE_v = valence band discontinuity expressed in volts

L_n = electron diffusion length in the p-type material

L_p = hole diffusion length in the n-type material

t_1 = thickness of the n-type material (surface layer)

d = thickness of the p-type material (base region)

τ_{01}, τ_{02} = minority carrier lifetimes in the depletion regions on the two sides of the junction

n_{i1}, n_{i2} = intrinsic carrier concentrations in the two semiconductors

ℓ_1, ℓ_2 = depletion layer widths at no bias (v=0) in the two semiconductors

k_1, k_2 are given by $k_1 = \left(1 + \frac{N_1 \epsilon_1}{N_2 \epsilon_2}\right)^{-1}$ and $k_2 = 1 - k_1$, where N_1, N_2, ϵ_1 and ϵ_2 are the impurity concentrations and dielectric constants of the two semiconductors

ϕ is given by $\tanh\phi = \frac{sL_p}{D_p}$ where s is the surface recombination velocity for semiconductor no. 1 (assumed to be n-type) and D_p is the hole diffusion constant

It should be noted that J_{rgo} in equation (1) is dependent on applied voltage V as given by equation (2). This happens because the widths of the depletion regions, as well as the electric field strength in these regions, depend on applied voltage. For equation (2) it was assumed that the junction is of step type.

(5) The theoretical efficiency for solar energy conversion is computed for (a) the ideal conditions of no reflection loss, 100% collection and no series resistance; (b) the ideal case with loss due to surface contact area included; (c) as (b) but with loss due to reflection and imperfect collection included; and (d) as (c) but with the effect of series resistance included.

(6) For comparison, similar computations are performed for Si and GaAs homojunction solar cells with physical parameters similar to those of practical solar cells.

2. DIODE GEOMETRY

All the solar cells considered are assumed to be of the same area ($1x2cm^2$) and have a surface contact made of the grid structure shown in Fig. 2. This grid structure was selected because it is commonly used for Si solar cells (Handy, 1967). In this configuration, approximately 12.8 percent surface area is covered by the contacts.

3. COMPUTATION OF REFLECTION LOSS

Since the refractive index of most of the semiconductors is high (for Si, $n \simeq 3.5$), the reflection loss from the surface of the photocell is prohibitive unless some kind of anti-reflection film is used. The refractive index is represented in complex notation as n-ik, where n and k are related to the reflection coefficient ρ and absorption coefficient α by

$$k = \frac{\alpha \lambda_o}{4\pi} \tag{4}$$

$$n = \frac{1+\rho}{1-\rho} + \sqrt{\left(\frac{1+\rho}{1-\rho}\right)^2 - (1+k^2)} \tag{5}$$

where λ_o is the wavelength of light in free space. For a heterojunction cell, one has to consider in principle an additional reflecting surface at the n-p junction. In practice, however, this complex situation may be simplified by assuming that the first semiconductor layer is thick for optical computations. This may be justified (Vasicek, 1960) by showing that the path difference in the first semiconductor $2n_1t_1$ is greater that 5 λ_o. This allows us to first compute the composite reflection coefficient of the heterojunction cell and then take into account the reduction in reflection caused by a transparent (k=0) antireflection film. The formulae to be used for computing overall reflection (R) and transmission (T) into the second semiconductor material are:

$$R = \frac{R_o+R_{12}+2\sqrt{R_oR_{12}}\cos(4\pi n_ot_o/\lambda_o)}{1+R_oR_{12}+2\sqrt{R_oR_{12}}\cos(4\pi n_ot_o/\lambda_o)} \tag{6}$$

$$T = \frac{(1-R_o)(1-R_1)(1-R_2)e^{-4\pi k_1t_1/\lambda_o}}{(1-R_1R_2e^{-8\pi k_1t_1/\lambda_o})(1+R_oR_{12}+2\sqrt{R_oR_{12}}\cos(4\pi n_ot_o/\lambda_o)} \tag{7}$$

where

$$R_o = \left(\frac{n_o-1}{n_o+1}\right)^2 \quad , \quad R_1 = \frac{(n_1-n_o)^2+k_1^2}{(n_1+n_o)^2+k_1^2} \quad , \quad R_2 = \frac{(n_1-n_2)^2+(k_1-k_2)^2}{(n_1+n_2)^2+(k_1+k_2)^2}$$

$$R_{12} = \frac{R_1+(R_2-2R_1R_2)e^{-8\pi k_1t_1/\lambda_o}}{1-R_1R_2e^{-8\pi k_1t_1/\lambda_o}} \tag{8}$$

The subscripts o, 1 and 2 refer to the antireflection film, first semiconductor and second semiconductor respectively. R_{12} denotes the

composite reflection value for regions 1 and 2. The equations (6) and (7) were derived by following the approach of Vasicek (1960).

Since n and k for all the materials are functions of the wavelength of the light, the design of an antireflection film for a heterojunction solar cell should be based on maximizing the overall number of solar photons transmitted into the second semiconductor. For the homojunction cells considered, the optimum antireflection layer thickness, t_o, was selected by maximizing the total photons transmitted into the cell. Fig. 3 shows typical variation of transmission as a function of anti-reflection film thickness for ZnSe-GaAs and GaAs-GaAs cells. The solar spectrum considered in these calculations was that given by Moon (1940) for above atmosphere conditions. The optimum thickness of antireflection film is seen to be about 800 A° for the ZnSe-GaAs cell and about 700 A° for the GaAs-GaAs cell. Table I lists the optimum values for SiO and SiO_2 films for other heterojunction pairs considered and SiO is seen to be preferable for all pairs. In the studies that follow, all the cells being compared were therefore assumed to be coated with SiO of optimum thickness. The spectral response of the anti-reflection coating will be seen in curves (Fig. 5 and 6) that are presented in a later section on collection efficiency.

4. COMPUTATION OF COLLECTION EFFICIENCY AND SPECTRAL RESPONSE

As shown in Fig. 2(b), the solar cell under consideration consists of a surface n-layer and a base p-region. Since in heterojunctions, the absorption characteristics of the two regions are different, they will be treated separately.

TABLE I

OPTIMUM VALUES FOR ANTI-REFLECTION FILM THICKNESS

Solar Cell Material	SiO Film		SiO_2 Film		Reflection Loss* Without Any Film
	Optimum Thickness Angstroms	Reflection* Loss	Optimum Thickness Angstroms	Reflection* Loss	
ZnSe-Ge	950	11.22%	1275	12.24%	32.13%
ZnSe-GaAs	800	4.92%	1075	6.32%	25.88%
GaP-Si	900	8.62%	1200	12.5 %	30.35%
GaAs-Ge	1300	14.35%	1500	18.07%	34.22%
GaAs-GaAs	700	7.87%	950	14.9 %	36.6 %
Si-Si	800	10.12%	1050	16.07%	35.45%

* Reflection loss values are for the complete usable energy range of the sun's spectrum for the solar cell, viz. for $h\nu > Eg_{small}$

4.1 Holes in the n-Layer

The minority carrier (hole) diffusion equation under constant mono-energetic illumination is

$$D_p \frac{d^2p}{dx^2} - \frac{p-p_o}{\tau_p} + \alpha_1 N e^{-\alpha_1 x} = 0 \tag{9}$$

where p_o is the equilibrium hole concentration, τ_p is the hole lifetime, α_1 is the absorption coefficient (a function of wavelength), N is the number of photons entering the surface layer and x is measured from the n semiconductor surface as shown in Fig. 4a. If N_s represents the photon density in the sun's spectrum at that wavelength, then

$$N = N_s(1-R) \tag{10}$$

The boundary conditions for solving equation (9) are

$$D_p \frac{dp}{dx} = s(p-p_o) \text{ at } x = 0$$

and

$$p = p_o e^{qV/kT} \quad \text{at } x = t_1 - \ell_1 = t'$$

where s is surface recombination velocity and V is the bias voltage across the diode. Then the solution for the photo-current density collected from the undepleted n layer by diffusion, under short-circuit voltage conditions, is

$$J_S^P = q\left[\frac{N\alpha_1^2 L_p}{\alpha_1^2 L_p^2 - 1}\left\{\frac{D_p + s/\alpha_1}{D_p + sL_p} e^{-t'/L_p} - e^{-\alpha_1 t'}\right\} + \frac{N\alpha_1 L_p \tanh\left(\frac{t'}{L_p} + \phi\right)}{\alpha_1^2 L_p^2 - 1}\right.$$

$$\left.\left\{\frac{\alpha_1 L_p (D_p + s/\alpha_1)}{D_p + sL_p} e^{-t'/L_p} - e^{-\alpha_1 t'}\right\}\right] \tag{11}$$

Each photon absorbed in the depletion region is assumed to contribute one current carrier, and therefore the photo-current density due to the depletion region is given by

$$J_{DR}^{p} = qN(e^{-\alpha_1 t'} \quad e^{-\alpha_1 t}) \tag{12}$$

4.2 Electrons in the p-Region

Fig. 4(b) represents the coordinate system used for the p region. The diffusion equation for this region is then

$$D_n \frac{d^2 n}{dx^2} - \frac{n-n_o}{\tau_n} + \alpha_2 N^1 e^{-\alpha_2 x} = 0 \tag{13}$$

where α_2 is the absorption coefficient of the p base region and N^1 is the photon density transmitted into the base region, as given by

$$N^1 = N_s T \tag{14}$$

The boundary conditions are

$$n = n_o e^{qV/kT} \quad \text{at } x = \ell_2$$

and $n = n_o$ at $x = d$

Then the solution for the photo-current density due to absorption and diffusion in the undepleted base layer is

$$J_B^n = q\left[\frac{\alpha_2 N^1 e^{-\alpha_2 \ell_2}}{\alpha_2 + 1/L_n} - \frac{2\alpha_2 N^1 e^{-\alpha_2 \ell_2}(e^{-d/L_n} - e^{-\alpha_2 d})}{(\alpha_2^2 - 1/L_n^2)(e^{d/L_n} - e^{-d/L_n})}\right] \tag{15}$$

The photo-current density due to absorption in the base depletion region is

$$J_{DR}^{n} = qN^1 (1-e^{-\alpha_2 \ell_2}) \tag{16}$$

The total photo-current density of the solar cell is given by

$$J_T = J_S^p + J_{DR}^p + J_B^n + J_{DR}^n \qquad (17)$$

The various components of the photo current are obtained by integration over the photon energy range of interest ($h\nu > Eg$) for the region under consideration. The spectral response, i.e. the number of electrons collected per incident photon, and the total photo-current collected by the junction were computed for various heterojunction pairs. The spectral response of a ZnSe-GaAs heterojunction (cell B-1) is shown in Fig. 5. The contribution of the ZnSe layer is zero since the collection for photon energies greater than the ZnSe band gap is negligible. The contributions of the bulk base region and the base layer depletion region are also shown separately in Fig. 5. For this cell the base depletion region at zero voltage was 458 angstroms wide. Fig. 6 shows the spectral response of a comparable GaAs homojunction cell (cell F-1). The contributions of the n GaAs region and the pGaAs base region are also shown separately in Fig. 6. Comparison of Fig. 5 and 6 shows that the collection in the pGaAs is higher for the heterojunction cell, as might be expected, since there is no absorption in the window region. However, the heterojunction cell suffers a cutoff at the band gap of the ZnSe.

The surface layer, base layer and total collection efficiencies of various solar cells are given in Table II. The "window effect" is quite beneficial for the ZnSe-GaAs cell relative to GaAs-GaAs solar cells. For the GaP-Si heterojunction cells, relative to Si-Si cells, the collection efficiency is low, primarily because the optical absorption edge of Si is not sharp and the surface recombination velocity of Si can be controlled

TABLE II

COLLECTION EFFICIENCIES OF VARIOUS REGIONS OF SOLAR CELLS

Solar Cell	Cell†	Surface Layer Collection Efficiency * Percent	Base Layer Collection Efficiency ** Percent	Total Collection Efficiency*** Percent
ZnSe-Ge	A-1	0	97.3	87.8
n-p	A-2	0	97.3	84.2
ZnSe-GaAs	B-1	0	87.3	72.3
n-p	B-2	0	86.7	69.6
GaP-Si	C-1	1.4	84.9	74.8
n-p	C-2	.007	83.2	65.9
Si-Si	D-1	96	83.9	86.2
n-p	D-2	87.1	82	83.4
GaAs-Ge	E-1	58.6	96.1	83.2
n-p	E-2	41.8	95.7	74.2
GaAs-GaAs	F-1	58.5	84.4	64.3
n-p	F-2	41.0	77.8	45.1
p-n	G-1	53.6	75.8	58.5
	G-2	29.5	68.1	33.8

† The parameters assumed for the cells are given in Appendix A.

* Relative to the number of photons of the solar spectrum absorbed in the surface layer with $h\nu > E_{g2}$

** Relative to the solar photons entering the base layer with $h\nu > E_{g2}$

*** Relative to the number of photons of the solar spectrum entering the surface layer with $h\nu > E_{g2}$

to low values (10^3 cm/sec as compared to 10^5 cm/sec assumed for GaAs). However when series resistance effects are taken into account (in a later section) the window effect is found to lower the series resistance of the GaP-Si cell and bring up the power efficiency to a level comparable to that of Si-Si homojunction cells.

Table II also includes data on nZnSe-pGe and nGaAs-pGe solar cells. These pairs have good lattice-match conditions and minority carrier collection has been demonstrated in them. However Ge is not wide enough in band-gap to make these efficient solar cells, as we shall see later.

5. SERIES RESISTANCE CALCULATIONS

The major component of the series resistance of a solar cell is usually the resistance of the thin surface layer. In heterojunction cells the window effect allows one to increase the thickness of surface layer and thus reduce the series resistance. In order to make comparisons between different cells feasible, it is assumed that good-quality ohmic contacts can be made to the semiconductors so that the contact resistance is negligible. Internal resistance will thus be the sum of base region resistance and surface layer resistance. The base region resistance R_B is given by

$$R_B = \frac{\rho_B \, d}{A}$$

where ρ_B is base region resistivity and A is the area in cm^2 of the cell. For the geometry of Fig. 2, the area A is 2 cm^2.

Surface layer resistance was computed by the method described by Handy (1967). For the geometry shown in Fig. 2 we obtained for the surface

layer resistance R_S the following relations, in Handy's symbols,

$$R_S = \frac{R_c}{1+R_c/R_p} \tag{19}$$

where $$R_c = \frac{R_4\left(1+\dfrac{R_1}{R_3+R_{5/2}}+\dfrac{R_1}{R_1+R_4}\right)}{2+\dfrac{R_1+R_4}{R_3+R_{5/2}}}$$

$$R_p = \frac{R_c(R_c+R_1)}{2(2R_c+R_1)}$$

$$R_4 = \frac{\rho_s r_3}{t\ s}$$

$$R_5 = R_4\,\frac{r_3}{2W-r_3}$$

and r_3 is given by

$$\left(\frac{2r_3}{s}\right)^2 = \frac{2W}{r_3} - 1 - 2\left(\frac{W}{r_3}-1\right)^2 \log\left(\frac{W}{W-r_3}\right) \tag{20}$$

and ρ_s is the resistivity of the surface layer. For s equal to 0.4 cm and W as 0.9 cm, solution of equation (20) gives 0.26724 for the value of r_3. (The value of 0.37 as obtained by Handy appears to be in error. Also the equations to evaluate R_4 and R_5 are different because of different interpretation of some integrals involved). Values of R_1, R_3 and R_7 which are resistances of contact strip, grid strip and contact resistance of bottom electrode to bulk, were taken from Handy as 0.002, 0.4 and 0.08 ohms, respectively. The total series resistance R_T was computed as

$$R_T = R_B + R_S + R_1 + R_7 \tag{21}$$

Values of R_T for the cells under consideration are listed in Table III. They range from 0.183 to 1.752 ohms depending on the thickness of the window layer in the heterojunction cells. For the Si homojunction cells considered, the values were 0.561 and 0.958 ohms for two different cell proportions. This compares with a value of 0.72 ohms reported by Handy (1967) as measured for high efficiency n+p cells of this geometry.

6. SOLAR CELL EFFICIENCY CALCULATIONS

The I-V relationship of the solar cell can be represented by

$$I = A_{TOT}\left[J_{do}\left(e^{q(V-IR_T)/kT}-1\right)+J_{rgo}\left(e^{q(V-IR_T)/kT}-1\right)\right] - J_T \cdot A_{ACT} \tag{22}$$

where A_{TOT} and A_{ACT} are the total area and active area of the solar cell and J_T is the photo-current density collected by the junction under short-circuit conditions. A schematic representation of a solar cell delivering power to a load is given in Fig. 8. No simple analytical relationship between V and I can describe the maximum power point of the I-V relationship given by equation (22). Therefore, for each cell the I-V characteristic was computed on a point by point basis and the maximum power point determined by examination. The current and voltage at this point, denoted by I_{mp} and V_{mp}, along with the overall solar power conversion efficiency η_o are listed in Table III. This overall efficiency, which includes the major loss terms, is given by

$$\eta_o = \frac{V_{mp}\ I_{mp}}{.139 \times 2} \times 100 \text{ percent} \tag{23}$$

where 0.139 is the solar energy density in watt/cm^2 incident on the cell, and 2 cm^2 is the total area of the cell.

Included also in the Table are calculated efficiencies for each cell with relaxation of various loss terms. These higher efficiencies are given to compare with prior treatments where such simplifications have been made, and because they do represent certain upper bounds. However they are not achievable in practice and attention in our discussion will be centered mainly on the η_o values.

TABLE III

Solar Energy Conversion Efficiencies of Solar Cells

Solar Cell	Cell	R_T Ohms	Solar Cell Efficiency *				V_{mp} Volt	I_{mp} mA	$\frac{V_{mp}}{V_{oc}}$
			Practical, η_o	η_1	η_2	η_3			
ZnSe-GaAs n-p	B-1	.403	13.35	13.66	16.76	20.1	.814	45.63	.88
	B-2	.422	12.8	13.09	16.71	20.1	.809	44.C	.88
GaAs-GaAs n-p	C-1	.51	10.32	10.6	18.28	22.8	.733	39.14	.87
p-n	G-1	.933	10.48	10.9	20.73	22.8	.82	35.52	.87
GaP-Si n-p	C-1	1.752	10.15	12.5	13.40	17.2	.471	59.93	.73
	C-2	.183	10.74	10.94	13.40	17.2	.553	54.0	.86
Si-Si n-p	D-1	.958	11.69	13.33	17.54	21.65	.477	68.2	.78
	D-2	.561	11.98	12.89	17.54	21.65	.499	66.8	.81
ZnSe-Ge n-p	A-1	.404	8.18	9.48	11.32	13.8	.244	93.0	.72
	A-2	.423	7.84	9.11	11.32	13.8	.241	90.6	.72
GaAs-Ge n-p	B-1	.501	6.77	8.1	11.75	17 †	.223	84.5	.70
	B-2	.321	6.45	7.14	11.75	17 †	.233	76.9	.74
$Al_{.4}Ga_{.6}As$-GaAs	H-1					24.3†			

* η_o includes series resistance loss and all other losses, except the interface recombination factors which are presently unknown for heterojunctions,

η_1 assumes the series resistance loss to be negligible (R_T=0),

η_2 assumes R_T=0 and no reflection loss and perfect collection in the window region

η_3 as for η_2 but without loss due to surface contact area i.e. A_{TOT} and A_{ACT} assumed to be both $2cm^2$.

† these η_3 values for GaAs-Ge and $Al_{.4}Ga_{.6}As$-GaAs are not comparable with the values above them. They are for complete collection $h\nu > E_{g2}$ rather than taking account of the narrow window effect. This supposes that collection from the surface layer is possible, which may be only partially true.

7. DISCUSSION

Results presented show that heterojunction solar cells can be hoped for with efficiencies, η_o, comparable to or even greater than the efficiencies obtainable with Si or GaAs homojunction cells. The treatment given, however, neglects junction interface recombination. This is a relatively unknown factor in heterojunction solar cells, since few acceptable structures have been made for study.

The theoretical results, with this proviso, show that nZnSe-pGaAs heterojunction solar cells should be capable of greater than 13% efficiency. This compares with about 10-1/2% for GaAs and 12% for Si homojunction cells, calculated on a similar basis. These values do not include the effects of built-in drift fields on cell performance. In practical Si cells this raises the measured performance to above 13%. A comparable improvement in nZnSe-pGaAs cells might be expected by the provision of a built-in field in the GaAs base region.

The output voltage of a ZnSe-GaAs cell at optimum load power is calculated to be in excess of 0.8 volts and the voltage decline between zero and full load power is 12%. Both of these values are better than for Si homojunction cells, for which the load voltage may be about 0.5 volts and the voltage regulation about 20%. Furthermore the ZnSe-GaAs cell should have an advantage over Si cells in performance at high temperatures, since the energy gap of GaAs is greater than that of Si.

GaP-Si heterojunction cells are also seen to be interesting from Table III, although the efficiencies expected are a little lower than for Si cells.

Another potential advantage of heterojunction cells is the possibility of low radiation damage in outer space conditions. Data is not readily available for effects of radiation damage in ZnSe, GaP and GaAs. However, in heterojunctions, when the surface layer is made thick enough and the window-region is utilized to create photo-carriers in the base region, the effect of radiation damage may be small, if the damage is confined mainly to the surface layer which does not contribute to the carrier collection. In Si homojunction cells, transparent covers are used to protect the cell from radiation damage. It is possible that these covers could be dispensed with in heterojunction cells having wide window regions.

ACKNOWLEDGMENTS

This work was supported in part by NASA Grant NGR 39-087-002. The authors gratefully acknowledge discussions with Dr. D. L. Feucht.

APPENDIX A

Table A and Table B list the various parameters used in computations for this work. Solar spectrum values were taken from Moon (1940). These values are very close to Johnson's values (Johnson, 1954) now used as standard for solar radiation. Complex refractive index values for GaAs and GaP were taken from the survey by Seraphin and Bennett (Willardson and Beer 1967). Diffusion lengths of minority carriers in GaAs were taken from Hwang (1969) and Rao-Sahib et al. (1969). Most other constants were taken from data sheets for semiconductors published by the Electronic Properties Information Center of Hughes Aircraft Company, Culver City, California.

TABLE A VALUES ASSUMED IN DESIGN CALCULATIONS

Solar Cell	Cell	t_o Angstroms	t_1 Microns	d Mils	s $cm\ sec^{-1}$	L_n Microns	L_p Microns	D_n $cm^2 sec^{-1}$	D_p $cm^2 sec^{-1}$	N_D cm^{-3}	N_A cm^{-3}	τ_n sec	τ_p sec
ZnSe-Ge n-p	A-1	950	7.5	20	10^5	707	.2	50	.5	10^{18}	10^{17}	10^{-4}	10^{-9}
	A-2	950	28	20	10^5	707	.3	50	1	2.10^{17}	10^{17}	10^{-4}	10^{-9}
ZnSe-GaAs	B-1	825	7.5	5	10^5	2.8	.2	80	.5	10^{18}	5.10^{17}	10^{-9}	10^{-9}
	B-2	825	28	5	10^5	2.8	.3	80	1	2.10^{17}	5.10^{17}	10^{-9}	10^{-9}
GaP-Si n-p	C-1	925	5	20	10^5	215	.3	23	1	10^{18}	2.10^{16}	2.10^{-5}	10^{-9}
	C-2	925	250	20	10^5	215	.3	23	1	10^{18}	2.10^{16}	2.10^{-5}	10^{-9}
Si-Si n-p	D-1	900	.5	20	10^3	215	1.7	23	3	10^{19}	2.10^{16}	2.10^{-5}	10^{-8}
	D-2	900	1	20	10^3	215	1.7	23	3	10^{19}	2.10^{16}	2.10^{-5}	10^{-8}
GaAs-Ge n-p	E-1	1300	.5	20	10^5	848	2	72	4	10^{18}	2.10^{16}	10^{-4}	10^{-8}
	E-2	1300	1	20	10^5	848	2	72	4	10^{18}	2.10^{16}	10^{-4}	10^{-8}
GaAs-GaAs n-p	F-1	750	.5	5	10^5	3.5	2	125	4	10^{18}	10^{16}	10^{-9}	10^{-8}
	F-2	750	1	5	10^5	3.5	2	125	4	10^{18}	10^{16}	10^{-9}	10^{-8}
GaAs-GaAs p-n (reversed)	G-1	750	.5	5	10^5	2.2	.7	5	4.5	10^{19}	5.10^{16}	10^{-9}	10^{-8}
	G-2	750	1	5	10^5	2.2	.7	5	4.5	10^{19}	5.10^{16}	10^{-9}	10^{-8}
$Al_{.4}Ga_{.6}As$-GaAs n-p	H-1					2.8	.16	80	2.5	2.10^{17}	5.10^{17}	10^{-9}	10^{-10}

TABLE B

MATERIAL PARAMETERS ASSUMED

Material	E_g eV	Electron Affinity eV	Density of States		n_i cm^{-3}	ϵ_r
			N_c cm^{-3}	N_v cm^{-3}		
ZnSe	2.67	4.09	1.75×10^{18}	1.16×10^{19}	2.39×10^{-4}	9.1
GaP	2.2	4.01	7.02×10^{18}	1.16×10^{19}	4.52	8.1
$Al_{.4}Ga_{.6}As$	1.85	4.0*	7.9×10^{17}	1.16×10^{19}	7.1×10^{4}	-
GaAs	1.4	4.07	4.7×10^{17}	1.5×10^{19}	5.3×10^{6}	12.5
Si	1.08	4.01	2.8×10^{19}	1.05×10^{19}	1.44×10^{10}	12
Ge	0.67	4.13	1.05×10^{19}	6×10^{18}	2.21×10^{13}	16

*Not well established. Values as low as 3.5 eV have been inferred from heterojunction studies.

REFERENCES

Handy, R. J. (1967) Solid State Electronics, Vol. 10, 765.

Hwang, C. J. (1969) J. Appl. Phys., Vol. 40, 3731.

Johnson, P. S. (1954) F. Meteor, Vol. 11, 431.

Kagan, M. B. and T. L. Lyubashevskaya (1967) Soviet Physics - Solid State, Vol. 1, 1091.

Moon, P. (1940) J. Franklin Inst., Vol. 230, 583.

Perlman, S. S. (1964) Advanced Energy Conversion, Vol. 4, 187.

Rao-Sahib et al., (1969) J. Appl. Phys., Vol. 40, 3745.

Rappaport and Wysocki (1961) Acta Electronica, Vol. 5, 364.

Sreedhar et al., (1969) IEEE Trans. on Electron Devices, Vol. ED-16, 309.

Vasicek, A. (1960) "Optics of Thin Films," North-Holland Publishing Company, 139.

Willardson, R. K. and A. C. Beer (1967) Semiconductors and Semimetals, Vol. 3, Chapter 12.

Wolf, M., (1960) Proc. IEEE , Vol. 48, 1246.

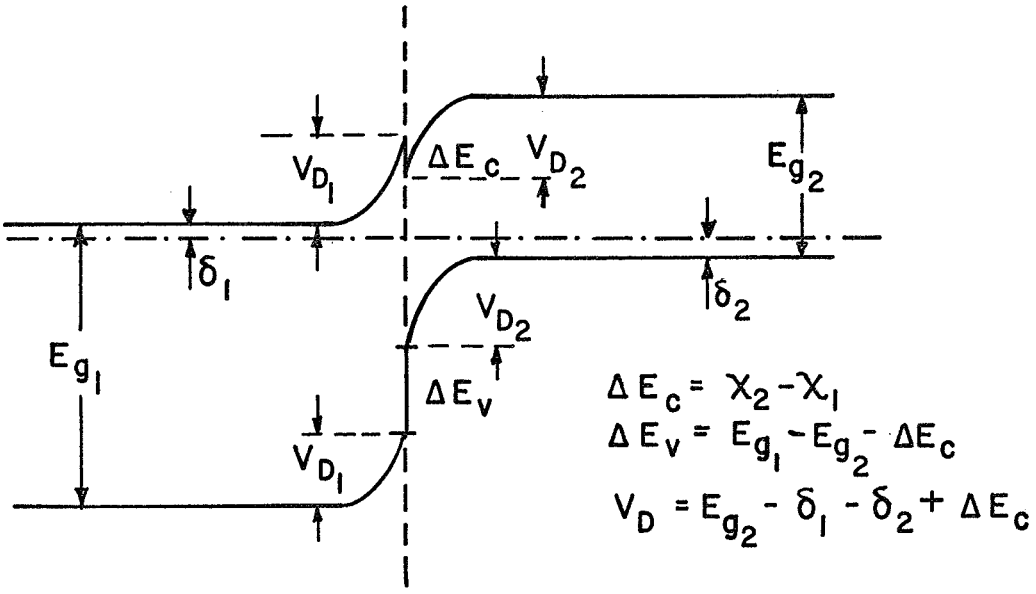

Fig. 1 Energy Band Diagram for an n-Window/p Base Heterojunction Solar Cell with No Light Applied

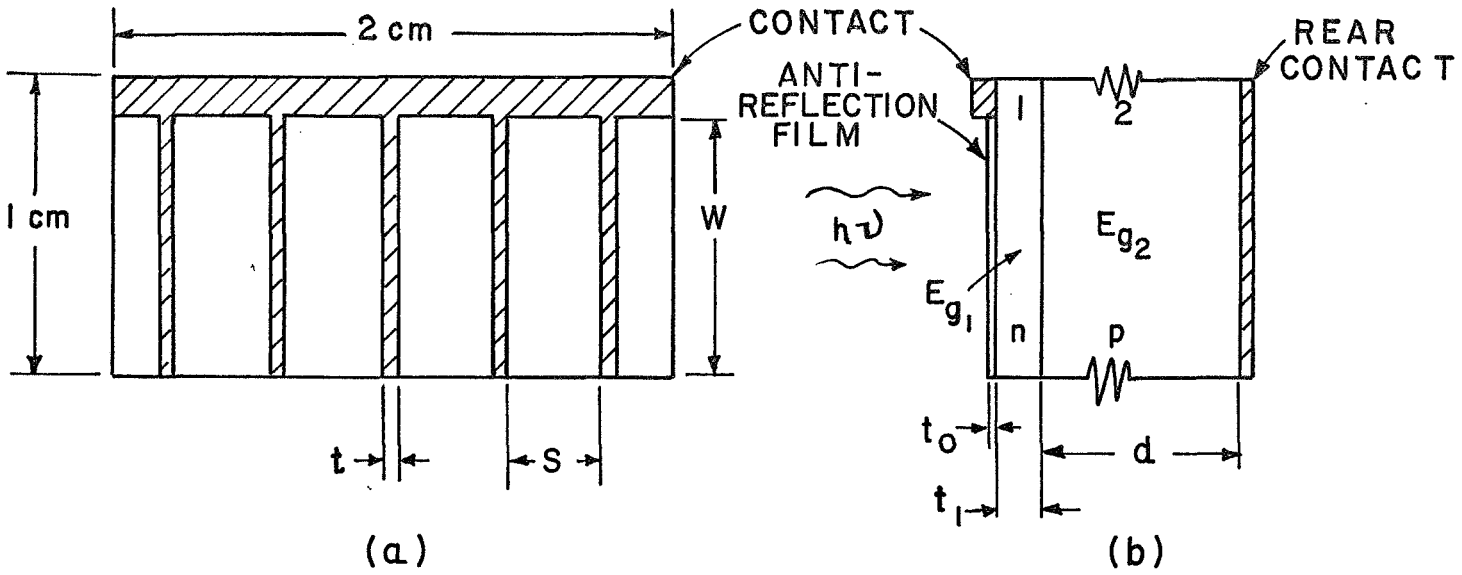

Fig. 2 Solar Cell Geometry Considered

(a) View of input face showing contact fingers:

W=0.9cm, S=0.4 cm, T=.0127 cm

(b) Cross-section

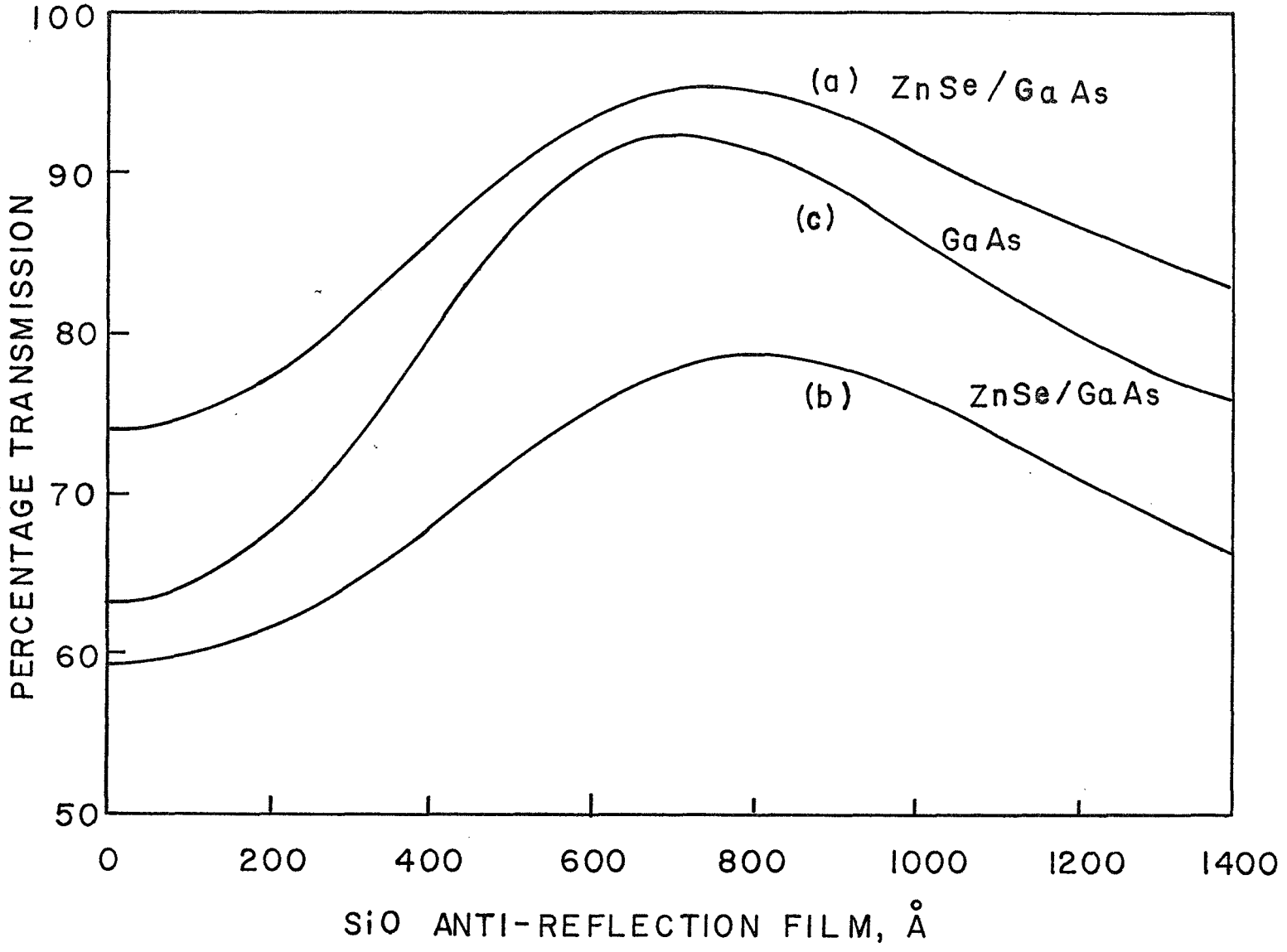

Fig. 3 Percentage Transmission of Solar Cell Spectrum as a Function of the SiO Anti-reflection Film Thickness

(a) Transmission into the surface layer (ZnSe) of a ZnSe-GaAs solar cell. The percentage represents the number of photons relative to the number in the full solar spectrum with $h\nu > 1.4$ eV.

(b) Transmission into the base layer of a ZnSe-GaAs cell. Curve (b) is lower than curve (a) because photons of energy greater than 2.67 eV do not reach the junction and there is an additional reflection at the junction interface.

(c) Transmission into the surface layer of a GaAs-GaAs solar cell (photons of energy greater than 1.4 eV) for comparison with curve (a).

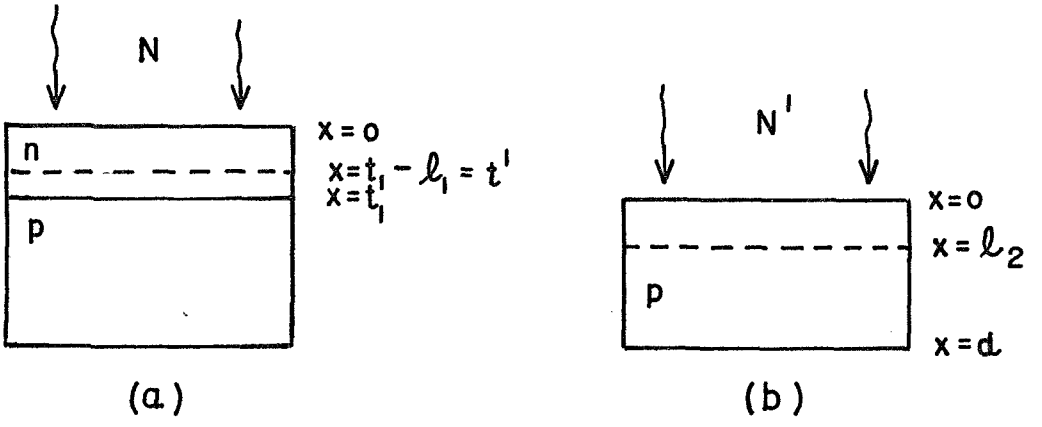

Fig. 4 Representation of Heterojunction Coordinates for Computation of Spectral Response of (a) Surface Layer (b) Base Region.

Lines at $x=t^{1}$ and $x = 1_2$ represent the two depletion edges of the junction.

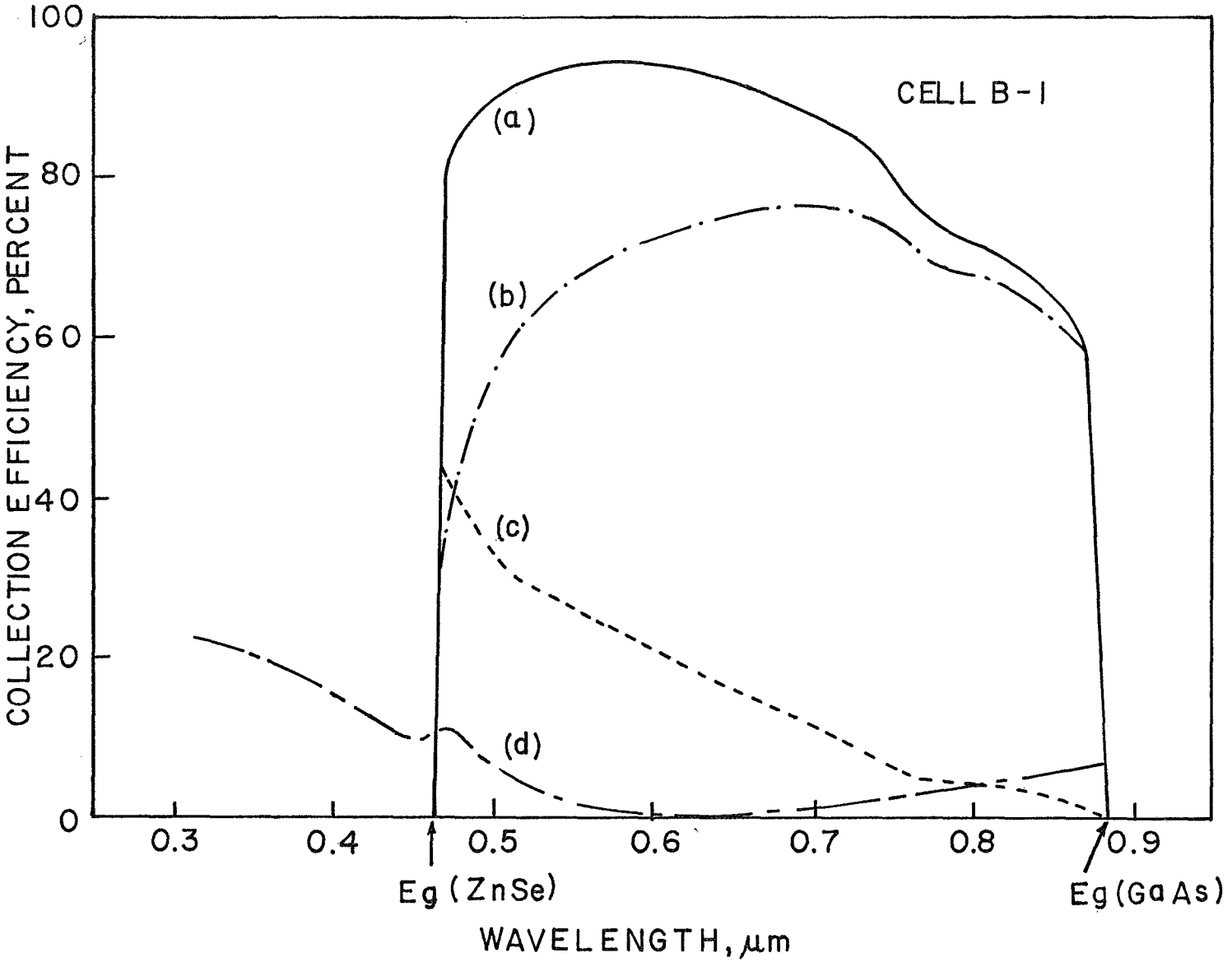

Fig. 5 Spectral Response of ZnSe-GaAs Heterojunction Solar Cell

(a) Computed collection efficiency (total)

(b) Bulk base region component of collection efficiency

(c) Base depletion layer component

(d) Reflection loss

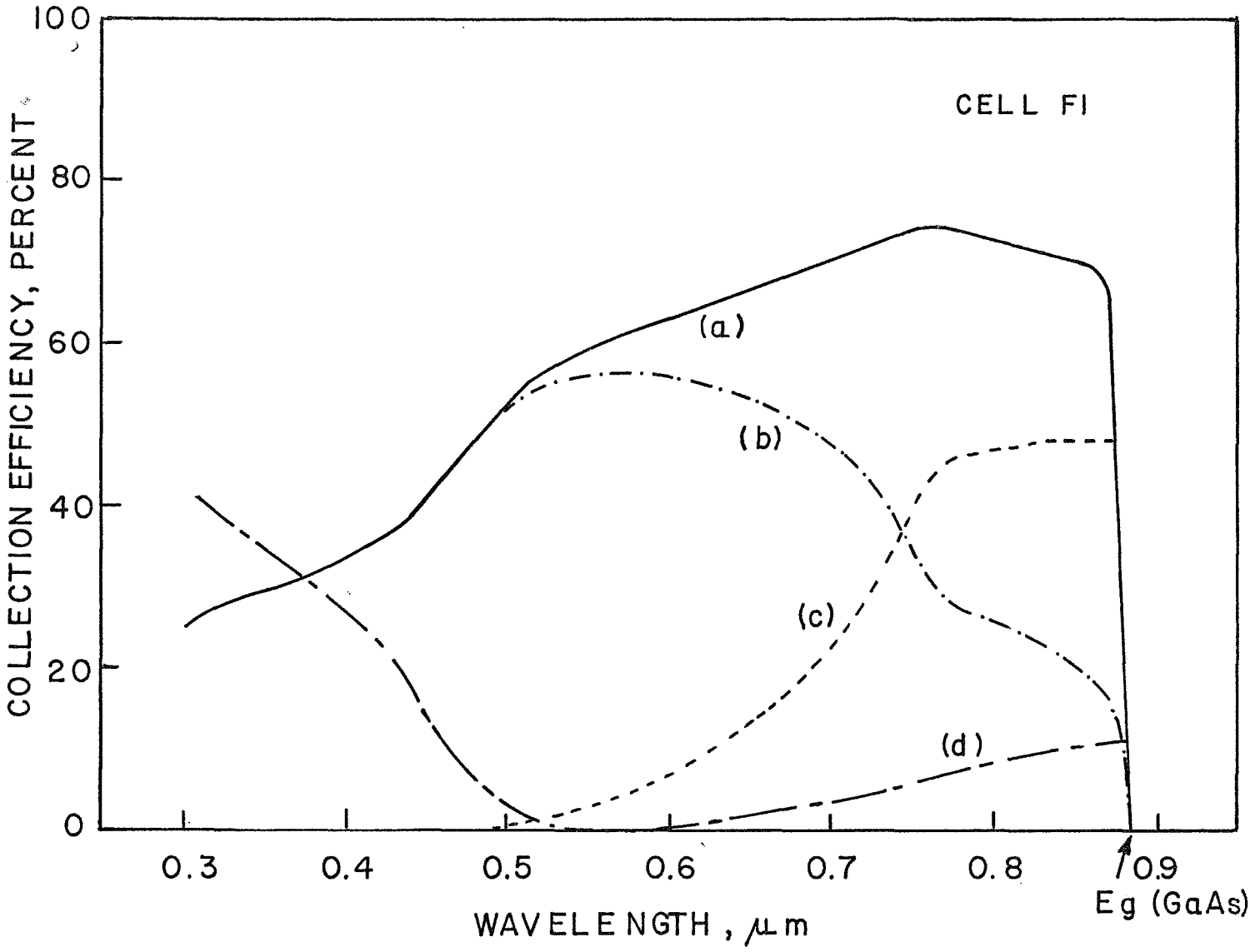

Fig. 6 Spectral Response of GaAs Homojunction Solar Cell

(a) Computed collection efficiency (total)

(b) Total base region response, pGaAs

(c) Response of the nGaAs layer

(d) Reflection loss

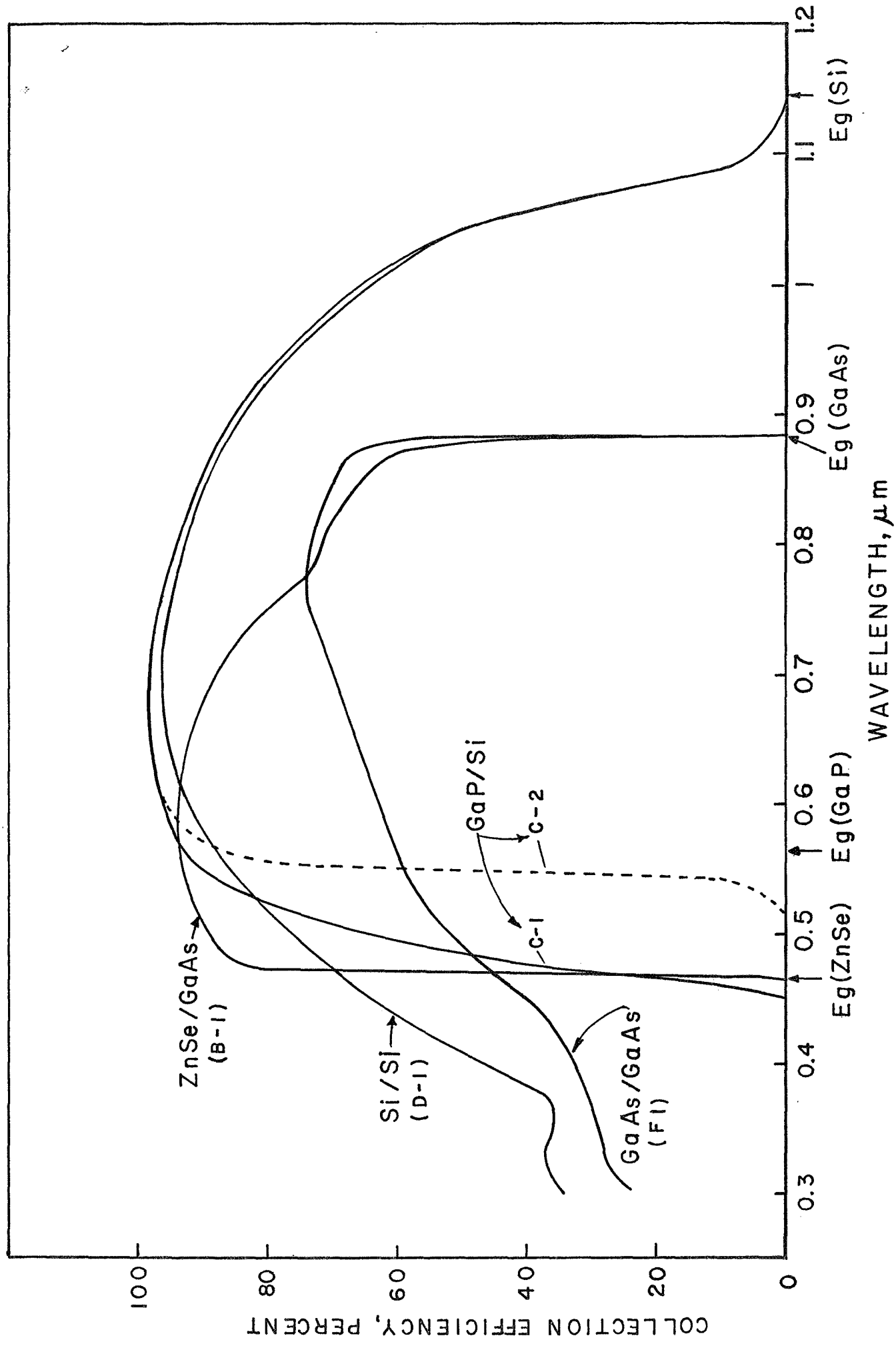

Fig. 7 Collection Efficiencies of Heterojunction and Homojunction Solar Cells

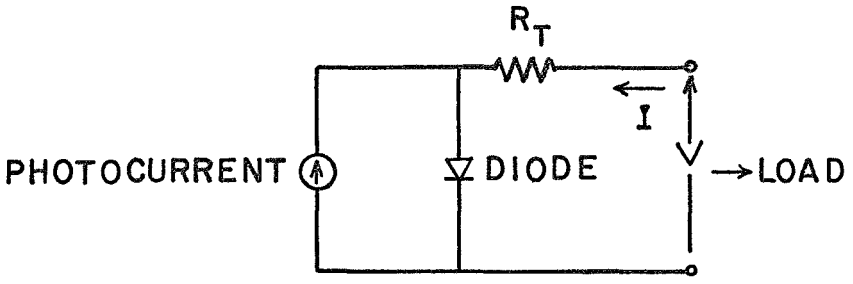

Fig. 8 Schematic Representation of Solar Cell Delivering Power to a Load.